5 Voltage Stability Margin Boundary Tracing

In Chapter 4 we discussed about various sensitivities that can be used to identify factors that may lead to voltage instability. In general these sensitivities are valid within the narrow range of parameter variation. This chapter provides the methodologies that extend the range of these parameter variations. The system load margin corresponding to any control configuration can be determined without retracing the entire PV curve.

5.1 Introduction

Deregulation brings new challenges to operate the power system. Independent System Operator (ISO) needs to monitor the system load margin in a real time and close the power transaction deals based on the available system stability margin as well as other considerations to meet the quickly varying energy demand. How to efficiently extend the system margin by the readjustment of the system control configuration becomes an important part of the overall operation of the power system.

Contingency causes system margin to shrink and could endanger a system. Hence load margin variation with respect to specified contingency could be a security index that can be applied in contingency screening [1] and operation planning.

Margin boundary can be obtained in a variety of ways. The trivial way to obtain a new margin point is to retrace the PV curve with changed system conditions. Obviously this method is time consuming and less informative.

As discussed in chapter 4 the boundary change can be estimated based on linear or quadratic margin sensitivity. With this approach tracing of the PV curve for each parameter change can be avoided. This leads to fast estimation of margin for changing conditions. But the prominent sources of inaccuracy inherently associated with margin sensitivity methods make a significant impact on the reliability of the margin estimation. In essence,

linear (or high order practically limited to no more than quadratic) sensitivity information is obtained by Taylor series expansion at the system margin point (critical point). Notice that the parameter change, sometimes due to contingency, may not be within a small range and hence higher nonlinearity could not be neglected [2]. Secondly, the effect of system limits may lead to discontinuous change in margin.

This chapter provides methodologies that can be used to estimate the margin for larger change in parameter values.

5.2 Natural Parameterization for Margin Boundary Tracing

As discussed in Chapter 3, power systems can be represented as a Differential and Algebraic Equation (DAE) model and is repeated here.

$$\begin{cases} \dot{X} = F(X,Y,U,Z) \\ 0 = G(X,Y,U,Z) \end{cases} \tag{5.1}$$

X contains all the system state variables; Y includes the algebraic variables; U is the control vector whereas Z consists of load variation at each bus.

Therefore the equilibrium manifold of power system is defined by [3]

$$\begin{cases} 0 = F(X,Y,U,Z) \\ 0 = G(X,Y,U,Z) \end{cases} \tag{5.2}$$

The solution set of above nonlinear equation system constructs a manifold, which could be parameterized by control parameters and disturbance parameters. Both X and Y indicate the state of the system, so they could be combined as state space. The parameter space is the combination of control parameters U and load parameters Z. There is a natural splitting in parameter space.

Parameter space = control parameter space $\oplus$ load parameter space

5.2.1 Load parameter space

As shown in Chapter 3, based on loading scenario, the loading parameter space could be parameterized by scalar λ to characterize the system loading pattern and the corresponding generation change.

$$\begin{cases} P_{Li} = (1 + K_{Li}\lambda)P_{Li0} \\ Q_{Li} = (1 + K_{Li}\lambda)Q_{Li0} \end{cases} \tag{5.3}$$

$$P_{Gi} = (1 + K_{Gi}\lambda)P_{Gi0} \tag{5.4}$$

As mentioned in Chapter 3, K_{Gi} is the generator load picking-up factor that could be determined by AGC, EDC or other system operating practice.

5.2.1 Control parameter space

Control parameter space can contain any type of control of interest. The following controls are studied in this chapter to demonstrate the concepts.

- Shedding loads
- Shunt capacitance
- Generator secondly voltage control

Control parameter space is parameterized by scalar β to characterize this space

$$U_i = U_{i0} + \beta K_{Ci} \tag{5.5}$$

Where U_{i0} indicates the initial configuration of control *i*.

Different combinations of control action can be achieved by assigning different ratio value to K_{Ci}.

This parameterization leads to two parameter variations: λ characterizing system loading condition with respect to a specified loading scenario and β characterizing control parameter with respect to a specified control scenario. The equations of power system are reduced to

$$\begin{cases} 0 = F(X, Y, \lambda, \beta) \\ 0 = G(X, Y, \lambda, \beta) \end{cases} \tag{5.6}$$

5.3 Formulation of Margin Boundary Tracing

5.3.1 Margin boundary manifold of power system

In the case of a multi-dimensional, implicitly defined manifold *M*, specific local parameterization needs to be constructed to trace a certain sub-manifold with special property on *M*. Saddle node or Hopf bifurcation point forms a margin boundary sub-manifold corresponding to the change of control parameters along a specified control scenario. Therefore bifurcation related stability margin boundary manifold could be traced by augmentation of power system equilibrium with characterization equation.

5.3.2 Characterization of margin boundary

5.3.2.1 Characterization of saddle node bifurcation related margin boundary tracing

Saddle node bifurcation of a dynamical system corresponds to co-dimension 1 fold bifurcation. As discussed in Chapter 3, a cut function for Saddle node related fold bifurcation can be implicitly defined as γ_{SNB} in the following equation

$$\begin{bmatrix} F_X & F_Y & e_k \\ G_X & G_Y & \\ e_j^T & & 0 \end{bmatrix} \begin{bmatrix} u_X \\ u_Y \\ \gamma_{SNB} \end{bmatrix} + \begin{bmatrix} 0 \\ 0 \\ 1 \end{bmatrix} = 0 \tag{5.7}$$

where we denote $u = \begin{bmatrix} u_X \\ u_Y \end{bmatrix}$, or equivalently

$$\begin{bmatrix} F_X & F_Y & e_k \\ G_X & G_Y & \\ e_j^T & & 0 \end{bmatrix}^T \begin{bmatrix} v_X \\ v_Y \\ \gamma_{SNB} \end{bmatrix} + \begin{bmatrix} 0 \\ 0 \\ 1 \end{bmatrix} = 0 \tag{5.8}$$

where we denote $v = \begin{bmatrix} v_X \\ v_Y \end{bmatrix}$.

With the formulation of (5.7), the cut set condition $\gamma_{SNB}(X,Y,u) = 0$ implies it is at the fold point.

If $\gamma_{SNB}(X,Y,u) = 0$, then

$$\begin{bmatrix} F_X & F_Y \\ G_X & G_Y \end{bmatrix} \begin{bmatrix} u_X \\ u_Y \end{bmatrix} = 0 \quad \text{and} \quad e_j^T \begin{bmatrix} u_X \\ u_Y \end{bmatrix} = 1$$

which implies $\begin{bmatrix} u_X \\ u_Y \end{bmatrix} \neq 0$ and $\begin{bmatrix} F_X & F_Y \\ G_X & G_Y \end{bmatrix}$ is singular.

For this condition $\begin{bmatrix} u_X \\ u_Y \end{bmatrix}$ is the right eigenvector associated with zero eigenvalue. Similarly $\begin{bmatrix} v_X \\ v_Y \end{bmatrix}$ is the left eigenvector associated with zero eigenvalue.

In principle, the indices k and j in (Eqs.5.7 and 5.8) may be kept fixed throughout the computation, but it is usually advantageous to update them occasionally by selecting new indices for the next step according to (Eqs.5.9 and 5.10)

$$\left|(e^k)^T v\right| = \max\left\{\left|(e^i)^T v\right|, i = 1,\cdots,m\right\} \tag{5.9}$$

$$\left|(e^j)^T u\right| = \max\left\{\left|(e^i)^T u\right|, i = 1,\cdots,m\right\} \tag{5.10}$$

5.3.3 Margin boundary tracing

5.3.3.1 Augmentation for bifurcation characterization

A characterization of bifurcation can be formulated in the cut set form on the solution manifold [4]. Our aim is trace the solution that is on the fold manifold. Solving equation (5.11) with condition (5.12) implies the solution of (5.11) is fold point.

We have to trace the solution of (5.11) for changing values of the load parameter λ and control parameter β. It becomes a two parameter variation problem

$$B(X,Y,u,\lambda,\beta)=\begin{bmatrix} F(X,Y,\lambda,\beta) \\ G(X,Y,\lambda,\beta) \\ \gamma_{SNB}(X,Y,u) \end{bmatrix}=0 \tag{5.11}$$

$$\gamma_{SNB}(X,Y,u)=\begin{bmatrix} F_X & F_Y \\ G_X & G_Y \end{bmatrix}\begin{bmatrix} u_X \\ u_Y \end{bmatrix}=0 \tag{5.12}$$

The following sections provide the basic approach to solve these set of equations using predictor and corrector continuation approach we discussed in chapter 3.

5.3.3.2 Augmentation for local parameterization

The total augmented equations for margin boundary tracing are

$$H(X,Y,u,\lambda,\beta)=\begin{bmatrix} B(X,Y,u,\lambda,\beta) \\ \begin{bmatrix} X^T & Y^T & \mu & \lambda & \beta \end{bmatrix} e_k-\eta \end{bmatrix}=[0] \tag{5.13}$$

$$=\begin{bmatrix} F(X,Y,u,\lambda,\beta) \\ G(X,Y,u,\lambda,\beta) \\ \gamma_{SNB}(X,Y,u) \\ \begin{bmatrix} X^T & Y^T & \mu & \lambda & \beta \end{bmatrix} e_k-\eta \end{bmatrix}=[0]$$

We can solve $H(X,Y,u,\lambda,\beta) = 0$ by applying predictor and corrector approach to (5.13) :

The margin boundary predictor is:

$$\frac{\partial H(X,Y,u,\lambda,\beta)}{\partial(X,Y,u,\lambda,\beta)}\begin{bmatrix} dX \\ dY \\ du \\ d\lambda \\ d\beta \end{bmatrix} = \begin{bmatrix} 0 \\ 0 \\ 0 \\ \pm 1 \end{bmatrix} \tag{5.14}$$

where

$$\frac{\partial H(X,Y,u,\lambda,\beta,)}{\partial(X,Y,u,\lambda,\beta,)} = \begin{bmatrix} \frac{\partial F}{\partial X} & \frac{\partial F}{\partial Y} & \frac{\partial F}{\partial u} & \frac{\partial F}{\partial \lambda} & \frac{\partial F}{\partial \beta} \\ \frac{\partial G}{\partial X} & \frac{\partial G}{\partial Y} & \frac{\partial G}{\partial u} & \frac{\partial G}{\partial \lambda} & \frac{\partial G}{\partial \beta} \\ \frac{\partial C}{\partial X} & \frac{\partial C}{\partial Y} & \frac{\partial C}{\partial u} & \frac{\partial C}{\partial \lambda} & \frac{\partial C}{\partial \beta} \\ & & e_k & & \end{bmatrix} \tag{5.15}$$

After solving (5.14) for a tangent vector, the predicted values of the unknown variables can be obtained from (5.15). Where δ is the step length

$$\begin{bmatrix} X_{pre} \\ Y_{pre} \\ u_{pre} \\ \lambda_{pre} \\ \beta_{pre} \end{bmatrix} = \begin{bmatrix} X \\ Y \\ u \\ \lambda \\ \beta \end{bmatrix}^{[i]} + \delta \begin{bmatrix} dX \\ dY \\ du \\ d\lambda \\ d\beta \end{bmatrix} \tag{5.16}$$

This predicted value can be used to as an initial guess to converge upon the margin boundary by solving the non-linear algebraic equations (5.13) with the Newton-Raphson method

Boundary corrector

Newton method is employed to do the boundary correction as

$$\begin{bmatrix} X \\ Y \\ u \\ \lambda \\ \beta \end{bmatrix}^{new} = \begin{bmatrix} X \\ Y \\ u \\ \lambda \\ \beta \end{bmatrix} - \left(\frac{\partial H(X,Y,u,\lambda,\beta)}{\partial(X,Y,u,\lambda,\beta)}\right)^{-1} H(X,Y,u,\lambda,\beta) \tag{5.17}$$

Iterate until the mismatch is less than the tolerance. Finally one can obtain the solution which is the fold point corresponding to $\lfloor X^T, Y^T, u, \lambda, \beta \rfloor e_k = \eta$

5.3.4 Basic Steps Involved in the Margin Boundary Tracing

The following steps are involved in margin boundary tracing.

1. Specify a loading scenario.
2. Equilibrium Tracing Program (EQTP) starts at current operating point for the first boundary point under current fixed control configuration and specified loading scenario.
3. Specify the control scenario that describes the change of control configuration or contingencies.
4. Predict the Boundary with Eq.5.16.
5. Correct the Boundary with Eq.5.17.
6. Go to step 4 unless some control variables hit limits, else stop.

5.3.5 Practical implementation

In the previous section saddle node bifurcation condition is explicitly included in the set of nonlinear equations. So when you solve these equations for changing load and control parameters the solution is always on the boundary. This formulation needs the second order derivatives. Another way to trace these boundaries is by extending EQTP discussed in Chapter 3. This approach is briefly explained through Fig.5.1.

For practical control variables range one may not encounter co-dimension 2 bifurcation (where the rank of the system Jacobian is n-2). In that case, a reduced method with only a one-dimension augmentation (unfolding) can

be easily employed to effectively trace voltage stability margin boundary. Nevertheless, since only one-dimension augmentation (unfolding) is applied, theoretically the reduced tracing method has a limited tracing range and could diverge near a co-dimension 2 saddle node bifurcation.

5.3.5.1 Implementation of reduced method

As for the power system equilibrium manifold in Eq.5.6, at first we fix the control at base value (β_0). Then

$$\begin{cases} 0 = F(X, Y, \lambda, \beta_0) \\ 0 = G(X, Y, \lambda, \beta_0) \end{cases}$$

When the system is not at a neighborhood of a co-dimension 2 saddle node bifurcation, the e_k in the second augmentation in Eq.5.13 could be set so that it always select λ as the continuation parameter. Then the problem turns into solving equation F, G, and cut function γ_{SNB} under different specified control conditions characterized by λ.

Notice that the previous margin boundary points are used as pivot (cut) condition to calculate the initial points of the part of equilibrium trajectory leading to the next margin boundary point defined by the new control parameter. Still the system load margin corresponding to a new control is determined without retracing the entire PV curve. Therefore the reduced margin boundary tracing is also computationally efficient. The procedure is as follows.

1. Under base control β_0 , use EQTP [5] and bifurcation identification conditions to trace to the SNB and then the initial margin boundary point is obtained.

$$\text{Predictor:} \begin{bmatrix} F_X & F_Y & F_\lambda \\ G_X & G_Y & G_\lambda \\ & e_j^T & \end{bmatrix}^{\beta_0} \begin{bmatrix} dX \\ dY \\ d\lambda \end{bmatrix} = \begin{bmatrix} 0 \\ 0 \\ \pm 1 \end{bmatrix} \tag{5.18}$$

$$\text{Corrector:} \begin{bmatrix} F_X & F_Y & F_\lambda \\ G_X & G_Y & G_\lambda \\ & e_j^T & \end{bmatrix}^{\beta_0} \begin{bmatrix} \Delta X \\ \Delta Y \\ \Delta \lambda \end{bmatrix} = -\begin{bmatrix} F^{\beta_0} \\ G^{\beta_0} \\ 0 \end{bmatrix} \tag{5.19}$$

Assume that the initial margin boundary point with load margin λ_0 under the base control β_0 is obtained.

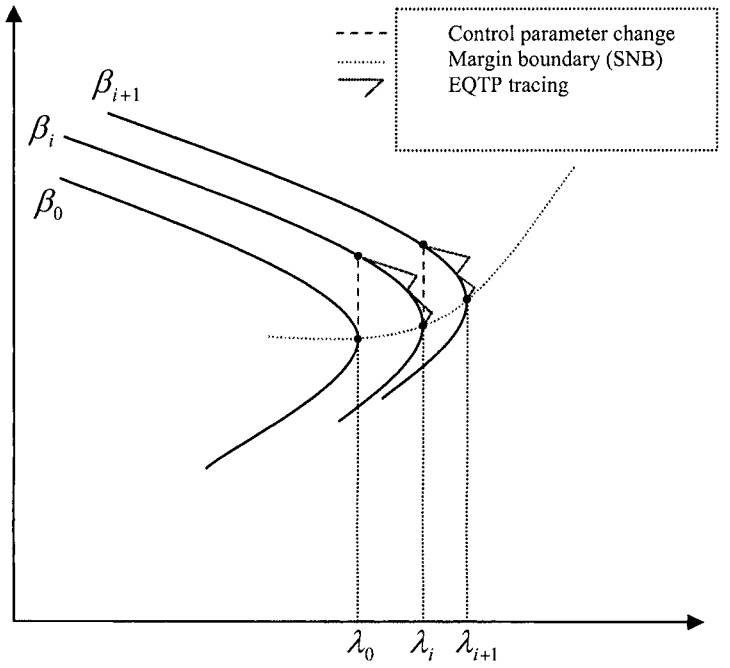

Fig. 5.1 Illustration of reduced implementation of margin boundary Tracing

2. Change the control parameter by a specified single step size δ. $\beta_{i+1} = \beta_i + \delta$.

3. With the jth element of the previous margin boundary point solution vector $[X^T \; Y^T \; \lambda_0]^T$ as the pivot (cut) condition, solve the following equations and use the solution as the initial point to trace the new equilibrium trajectory defined by the new control parameter.

4. From the new initial point, use EQTP and bifurcation identification conditions to trace the next SNB under the new control parameter β_{i+1}.

$$\text{Predictor:} \quad \begin{bmatrix} F_X & F_Y & F_\lambda \\ G_X & G_Y & G_\lambda \\ & e_j^T & \end{bmatrix}^{\beta_{i+1}} \begin{bmatrix} dX \\ dY \\ d\lambda \end{bmatrix} = \begin{bmatrix} 0 \\ 0 \\ \pm 1 \end{bmatrix} \tag{5.20}$$

$$\text{Corrector:} \quad \begin{bmatrix} F_X & F_Y & F_\lambda \\ G_X & G_Y & G_\lambda \\ & e_j^T & \end{bmatrix}^{\beta_{i+1}} \begin{bmatrix} \Delta X \\ \Delta Y \\ \Delta \lambda \end{bmatrix} = -\begin{bmatrix} F^{\beta_{i+1}} \\ G^{\beta_{i+1}} \\ 0 \end{bmatrix} \tag{5.21}$$

Then a new boundary point with margin λ_{i+1} under the new control parameter β_{i+1} is obtained (Note: the middle curve in the Fig.5.1 corresponds to the control β_i).

5. Repeat step 2-4 to obtain the margin boundary points until the studied controls hit their limits.

5.4 Examples

Two bus example:

For this example, the unity power factor is still used. Margin boundary tracing can be demonstrated with respect to shunt compensation and series compensation, respectively. The method described in section 5.3.3 is first utilized here to trace the margin boundary. Then, the method described in section 5.3.4 is applied for comparison. For simplification, only power flow equations are used.

(1) Shunt compensation at bus 2

The power flow equations of the 2-bus system are:

$$G_1(\delta, V_2, \underline{h}, \lambda, \beta) = 1.4(1+\lambda) + 10V_2 \sin(\delta) = 0$$

$$G_2(\delta, V_2, \underline{h}, \lambda, \beta) = -10V_2 \cos(\delta) + (10-\beta)V_2^2 = 0$$

where, β is the shunt capacitance at bus 2(p.u.).

Singularity conditions are shown as follows:

$$\begin{bmatrix} G_{1\delta} & G_{1V_2} \\ G_{2\delta} & G_{2V_2} \end{bmatrix}\begin{bmatrix} h_1 \\ h_2 \end{bmatrix} = \begin{bmatrix} 10V_2\cos(\delta) & 10\sin(\delta) \\ 10V_2\sin(\delta) & (20-2\beta)V_2 - 10\cos(\delta) \end{bmatrix}\begin{bmatrix} h_1 \\ h_2 \end{bmatrix} = \begin{bmatrix} 0 \\ 0 \end{bmatrix}$$

$$h_2 = 1.0$$

Since h_2 is a constant, we can replace it with 1.0.

$$1.4(1+\lambda) + 10V_2\sin(\delta) = 0$$
$$-10V_2\cos(\delta) + (10-\beta)V_2^2 = 0$$
$$10V_2\cos(\delta)h_1 + 10\sin(\delta) = 0$$
$$10V_2\sin(\delta)h_1 + [(20-2\beta)V_2 - 10\cos(\delta)] = 0$$

[Note: For this simple 2-bus example, we can also use Eq.5.7 to get the cut function for the bifurcation boundary; it can be used to replace the last two equations of the above set.

$$\gamma(\delta, V_2, \lambda, \beta) = 10 - (20-2\beta)V_2\cos(\delta) = 0\,]$$

Hence, the H matrix can be expressed as:

$$H = \begin{bmatrix} 10V_2\cos(\delta) & 10\sin(\delta) & 0 & 1.4 & 0 \\ 10V_2\sin(\delta) & (20-2\beta)V_2 - 10\cos(\delta) & 0 & 0 & -V_2^2 \\ -10V_2\sin(\delta)h_1 + 10\cos(\delta) & 10\cos(\delta)h_1 & 10V_2\cos(\delta) & 0 & 0 \\ 10V_2\cos(\delta)h_1 + 10\sin(\delta) & 10\sin(\delta)h_1 + 20 - 2\beta & 10V_2\sin(\delta) & 0 & -2V_2 \\ & & e_k^T & & \end{bmatrix}$$

Select β as the continuation parameter, then k=5.

Tangent vector is: $[d\delta \quad dV_2 \quad dh_1 \quad d\lambda \quad d\beta]^T$

Base case SNB point is (corresponding to $\beta = 0$, $P_0 = 0.14$, normalized value):

$$V_2 = 0.7071, \delta = -0.7854, \lambda = 2.5714, h_1 = 1.4142, P_{cri} = 0.5$$

Predictor step:

$$[d\delta \quad dV_2 \quad dh_1 \quad d\lambda \quad d\beta]^T$$
$$= [0.0079 \quad 0.0763 \quad -0.1302 \quad 0.3571 \quad 1.0]^T$$

Taking step length $\sigma = 0.1$, then:

$$[\delta^{pre} \quad V_2^{pre} \quad h_1^{pre} \quad \lambda^{pre} \quad \beta^{pre}]^T$$
$$= [-0.7846 \quad 0.7147 \quad 1.4012 \quad 2.6071 \quad 0.1]^T$$

Corrector step:

$$[\Delta\delta \quad \Delta V_2 \quad \Delta h_1 \quad \Delta\lambda \quad \Delta\beta]^T$$
$$= [-0.0008 \quad -0.0005 \quad -0.0012 \quad 0.0004 \quad 0]^T$$

$$[\delta^{new} \quad V_2^{new} \quad h_1^{new} \quad \lambda^{new} \quad \beta^{new}]^T$$
$$= [-0.7854 \quad 0.7142 \quad 1.40 \quad 2.6075 \quad 0.1]^T$$

Hence, the new margin is:

$$P_0 * (1 + \lambda^{new}) = 0.14 * (1 + 2.6075) = 0.5051$$

Applying the continuation Prediction-Correction method step by step, we can trace the saddle node bifurcation margin boundary with respect to β (shunt capacitance).

Furthermore, if we use the normalized equation, the analytical expression for the margin for this simple system is given in the reference [6]:

$$p^{new} = \frac{\cos(\varphi)}{1 + \sin(\varphi)} \frac{1}{1 - B_c X}$$

Where, B_c is the shunt capacitance at bus 2(p.u.).

The comparison results between analytical value and MBT approach with the intermediate steps are shown in table5.1 and fig5.2:

Table 5.1 Comparison results

Shunt2 (p.u.)	V_2 (p.u.)	h_1	λ	MBT (normz.)	Analytical (normz.)
0	0.7071	1.4142	2.5714	0.5	0.5
0.1	0.7142	1.4001	2.6075	0.505	0.50505
0.2	0.7215	1.3859	2.6443	0.5102	0.5102
0.3	0.729	1.3718	2.6819	0.5155	0.51546
0.4	0.7366	1.3576	2.7202	0.5208	0.52083
0.5	0.7443	1.3435	2.7594	0.5263	0.52632
0.6	0.7522	1.3294	2.7994	0.5319	0.53191
0.7	0.7603	1.3152	2.8402	0.5376	0.53763
0.8	0.7686	1.3011	2.882	0.5435	0.54348
0.9	0.777	1.2869	2.9246	0.5495	0.54945
1	0.7857	1.2728	2.9683	0.5556	0.55556
1.1	0.7945	1.2587	3.0128	0.5618	0.5618
1.2	0.8035	1.2445	3.0584	0.5682	0.56818
1.3	0.8128	1.2304	3.1051	0.5747	0.57471
1.4	0.8222	1.2162	3.1528	0.5814	0.5814
1.5	0.8319	1.2021	3.2017	0.5882	0.58824

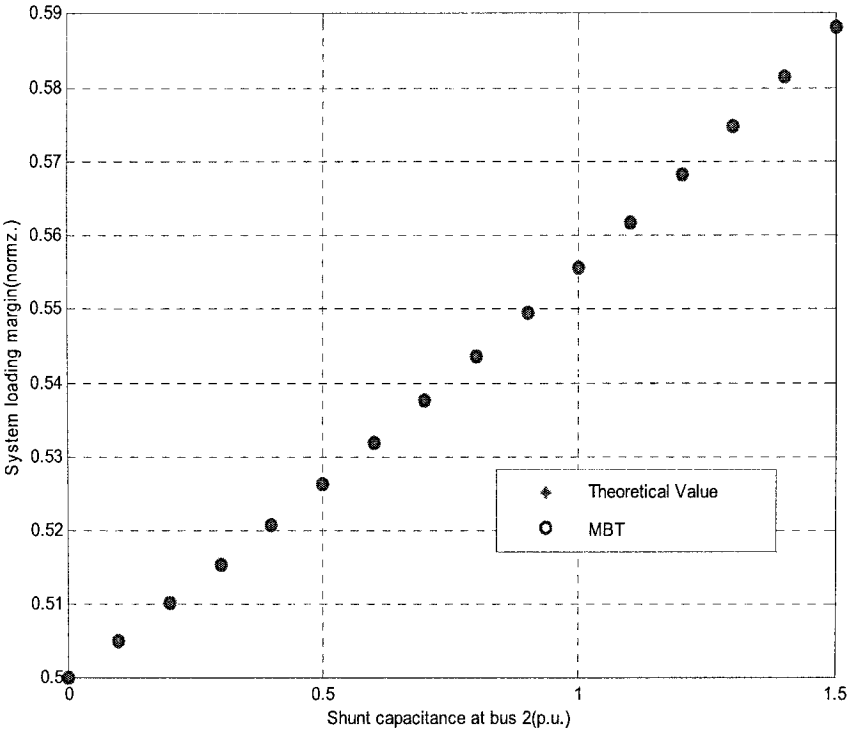

Fig. 5.2 System margin variation with shunt capacitance (analytical vs. MBT full)

Figure 5.3 shows the margin variation obtained through reduced formulation. These results are comparable.

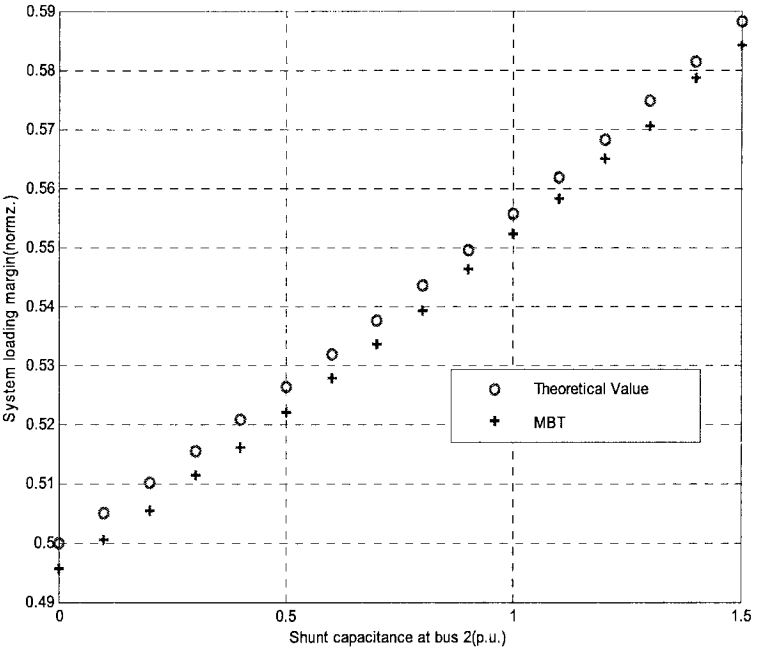

Fig. 5.3 System margin variation with shunt capacitance (analytical vs. MBT reduced)

(2) Series compensation between bus 1 and bus 2

The formulation is same as before except here β is equivalent total series admittance

$$G_1(\delta, V_2, \lambda, \beta) = 1.4(1+\lambda) + \beta V_2 \sin(\delta) = 0$$
$$G_2(\delta, V_2, \lambda, \beta) = -\beta V_2 \cos(\delta) + \beta V_2^2 = 0$$

Singularity conditions:

$$\begin{bmatrix} G_{1\delta} & G_{1V_2} \\ G_{2\delta} & G_{2V_2} \end{bmatrix} \begin{bmatrix} h_1 \\ h_2 \end{bmatrix} = \begin{bmatrix} \beta V_2 \cos(\delta) & \beta \sin(\delta) \\ \beta V_2 \sin(\delta) & 2\beta V_2 - \beta \cos(\delta) \end{bmatrix} \begin{bmatrix} h_1 \\ h_2 \end{bmatrix} = \begin{bmatrix} 0 \\ 0 \end{bmatrix}$$

$$h_2 = 1.0$$

The total set of equations to be solved:

$$
\begin{aligned}
&1.4(1+\lambda)+\beta V_2\sin(\delta)=0\\
&-\beta V_2\cos(\delta)+\beta V_2^2=0\\
&\beta V_2\cos(\delta)h_1+\beta\sin(\delta)=0\\
&\beta V_2\sin(\delta)h_1+2\beta V_2-\beta\cos(\delta)=0
\end{aligned}
$$

$$
H=\begin{bmatrix}
\beta V_2\cos(\delta) & \beta\sin(\delta) & 0 & 1.4 & V_2\sin(\delta)\\
\beta V_2\sin(\delta) & 2\beta V_2-\beta\cos(\delta) & 0 & 0 & V_2^2-V_2\cos(\delta)\\
-\beta V_2\sin(\delta)h_1+\beta\cos(\delta) & \beta\cos(\delta)h_1 & \beta V_2\cos(\delta) & 0 & V_2\cos(\delta)h_1+\sin(\delta)\\
\beta V_2\cos(\delta)h_1+\beta\sin(\delta) & \beta\sin(\delta)h_1+2\beta & \beta V_2\sin(\delta) & 0 & V_2\sin(\delta)h_1+2V_2-\cos(\delta)\\
 & e_k^T & & &
\end{bmatrix}
$$

Select β as the continuation parameter, then k=5.

Tangent vector is: $[d\delta \quad dV_2 \quad dh_1 \quad d\lambda \quad d\beta]^T$.

Base case SNB point is (corresponding to $\beta=10$, and $P_0=0.14$ is normalized value):

$$V_2=0.7071, \delta=-0.7854, \lambda=2.5714, h_1=1.4142, P_{cri}=0.5$$

Applying the continuation Prediction-Correction method step by step as shown before one can trace the saddle node bifurcation margin boundary with respect to β (series admittance).

The analytical expression of the margin for series compensation as given in reference [6] is:

$$P_{\max}=\frac{\cos(\varphi)}{1+\sin(\varphi)}\frac{E^2}{2X}=\frac{\cos(\varphi)}{2(1+\sin(\varphi))}E^2B$$

This relation shows that the margin changes linearly with respect to the change of equivalent total series admittance.

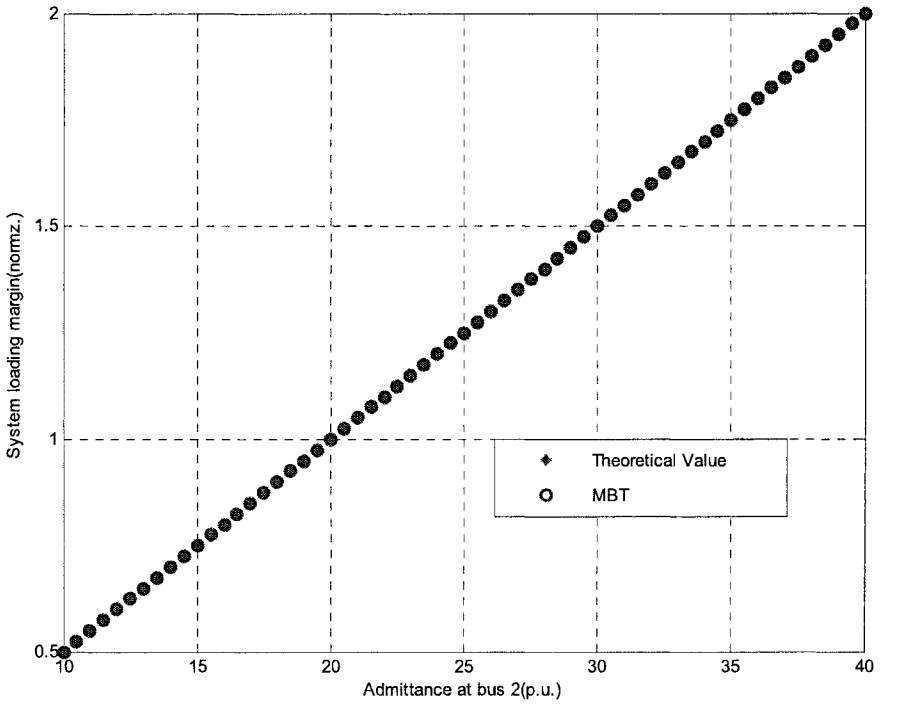

Fig.5.4 System margin variation with total equivalent series admittance (analytical vs. MBT)

Meanwhile, the degree of compensation can be calculated by:

$$X_c\% = (1 - \frac{B_0}{B_{new}}) * 100$$

If we use the $X_c\%$ as the parameter β instead, the power flow equations will be:

$$G_1(\delta, V_2, \lambda, \beta) = 1.4(1+\lambda) + \frac{1000}{100-\beta} V_2 \sin(\delta) = 0$$

$$G_2(\delta, V_2, \lambda, \beta) = -\frac{1000}{100-\beta} V_2 \cos(\delta) + \frac{1000}{100-\beta} V_2^2 = 0$$

And H changes into (using $m = \frac{1000}{100-\beta}, n = \frac{1000}{(100-\beta)^2}$ to simplify):

$$H = \begin{bmatrix} mV_2\cos(\delta) & m\sin(\delta) & 0 & 1.4 & nV_2\sin(\delta) \\ mV_2\sin(\delta) & mV_2\cos(\delta) & 0 & 0 & n(V_2^2 - V_2\cos(\delta)) \\ -mV_2h_1\sin(\delta)+m\cos(\delta) & m\cos(\delta)h_1 & mV_2\cos(\delta) & 0 & n[V_2\cos(\delta)h_1+\sin(\delta)] \\ mV_2\cos(\delta)h_1+m\sin(\delta) & m\sin(\delta)h_1+2m & mV_2\sin(\delta) & 0 & n[V_2\sin(\delta)h_1+2V_2-\cos(\delta)] \\ & & e_k^T & & \end{bmatrix}$$

The figure5.5 shows the change of system loading margin with respect to degree of compensation $X_c\%$:

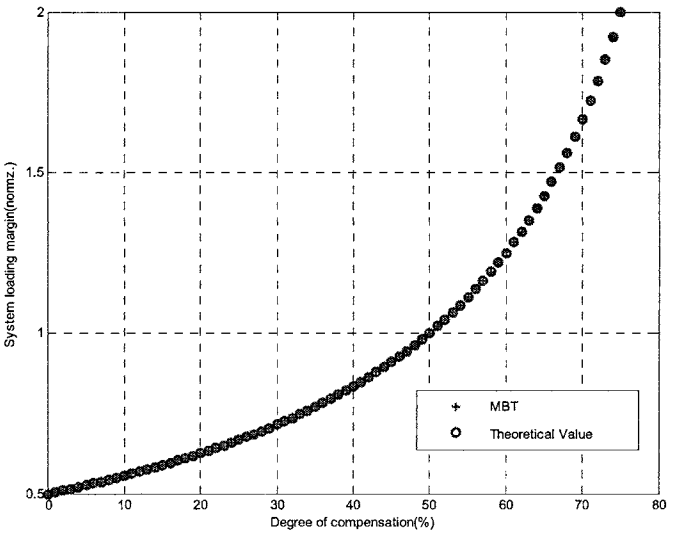

Fig.5.5 System margin variation with degree of compensation (analytical vs. MBT)

New England 39-bus system:

The following assumptions are made to demonstrate the boundary tracing on this test system

- Constant power load model;

- The maximum real power limit, the field current and the armature current limits are considered for each generator.
- No generator is allowed to have terminal voltage higher than 1.1 p.u., when its secondary voltage control is utilized to increase system stability margin;
- The loading scenario is defined as that all the loads are increased wit constant power factor, and all the generators participate in the load pick-up at the same rate.

The margin boundaries can be traced with respect to any specified control scenario.

5.4.1 Series compensation between bus 6 and bus 31

The figure5.6 shows the system loading margin change as the series admittance between bus 6 and bus 31 varies.

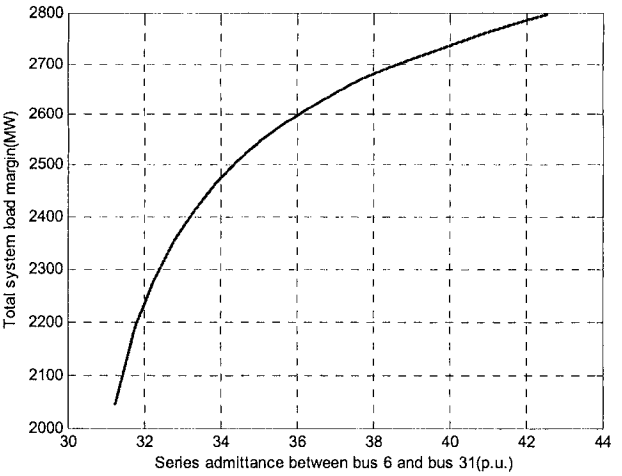

Fig. 5.6 System loading margin vs. series compensation

5.4.2 Shunt Compensation

Fig.5.7 shows the system loading margin change as shunt capacitance increases at bus 10.

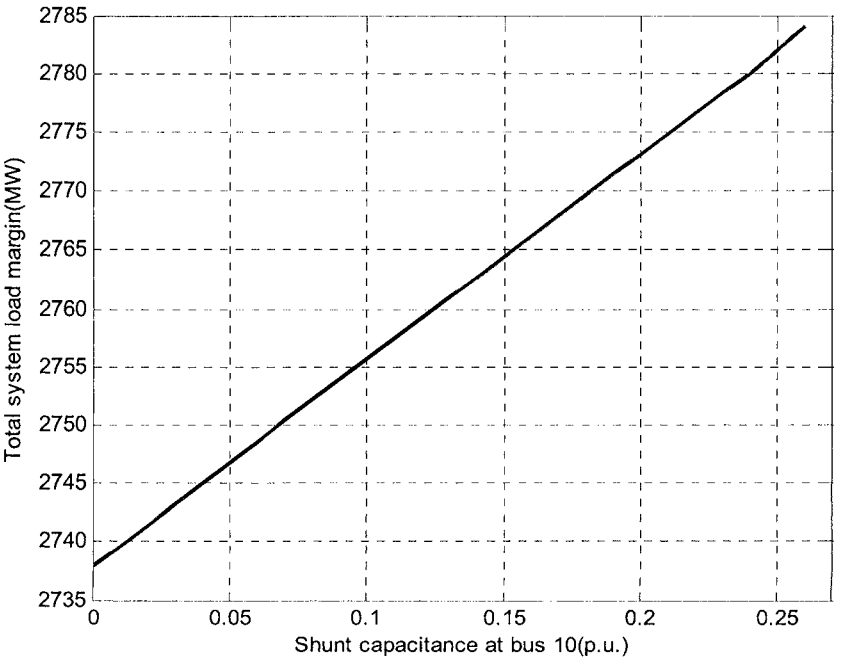

Fig. 5.7 System load margin vs. shunt capacitance at bus 10

5.4.3 Multiple contingencies

Voltage stability margin change due to single or multiple contingencies could also be traced by parameterizing the control parameter change involved in the contingency.

Let the $Y_{ij} = Y_{ij}^{(0)}(1-\beta)$ and $B_{ij} = B_{ij}^{(0)}(1-\beta)$. When the parameter β varying from zero to one, Y_{ij} and B_{ij} will vary from their initial values of $Y_{ij}^{(0)}$ and $B_{ij}^{(0)}$ to zero. Therefore, Y matrix becomes the post-contingency value.

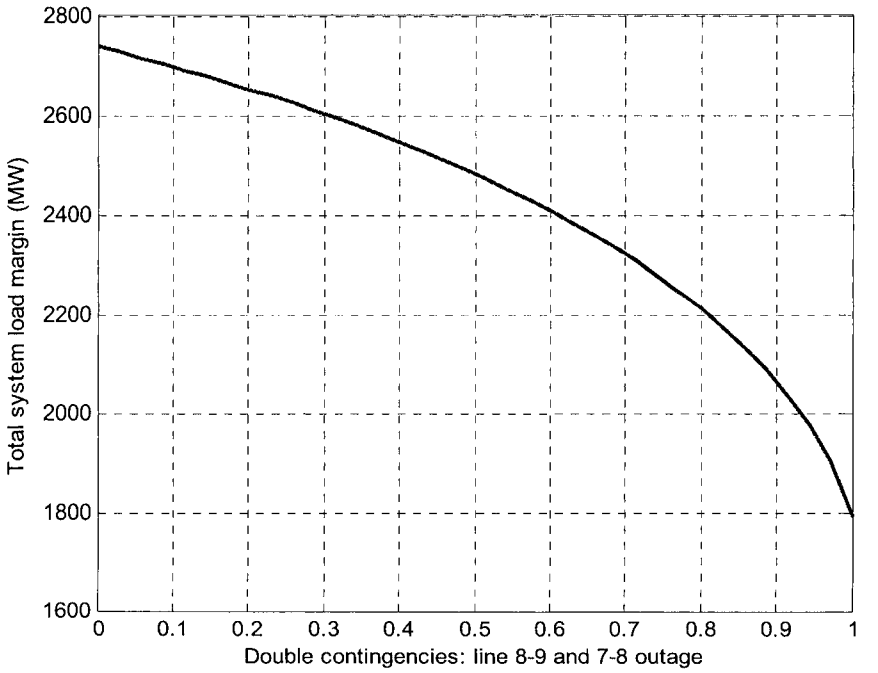

Fig. 5.8 System load margin vs. multiple contingencies: line 8-9 and line 7-8 outages

Fig. 5.8 shows the margin change for line outages. Zero indicates both line are in and one indicates both lines are out.

5.4.4 Boundary tracing with respect to generation control parameters

The margin boundaries can be traced with respect to any specified control scenario.

5.4.4.1 Load margin vs adjustment of Ka of AVR system

In Fig.5.9, voltage collapse (SNB related) margin boundary versus adjustment of Ka around its base case operating value is depicted as the solid curve.

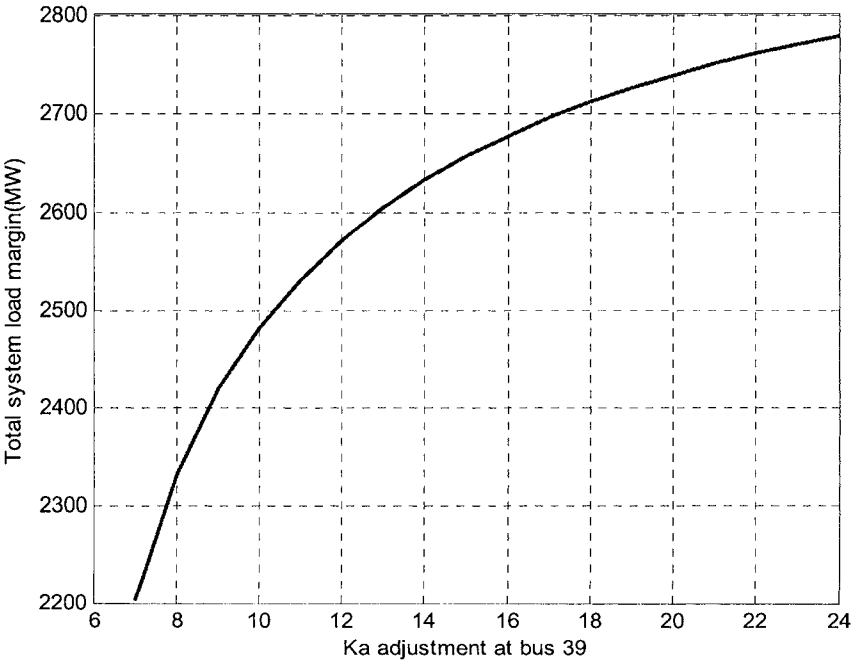

Fig. 5.9 margin boundary tracing vs. Ka adjustment

5.4.4.2 Load margin versus adjustment of V_{ref} of AVR system

Fig.5.10 shows the system voltage stability margin change with respect to the change of generator V_{ref} at bus 39.

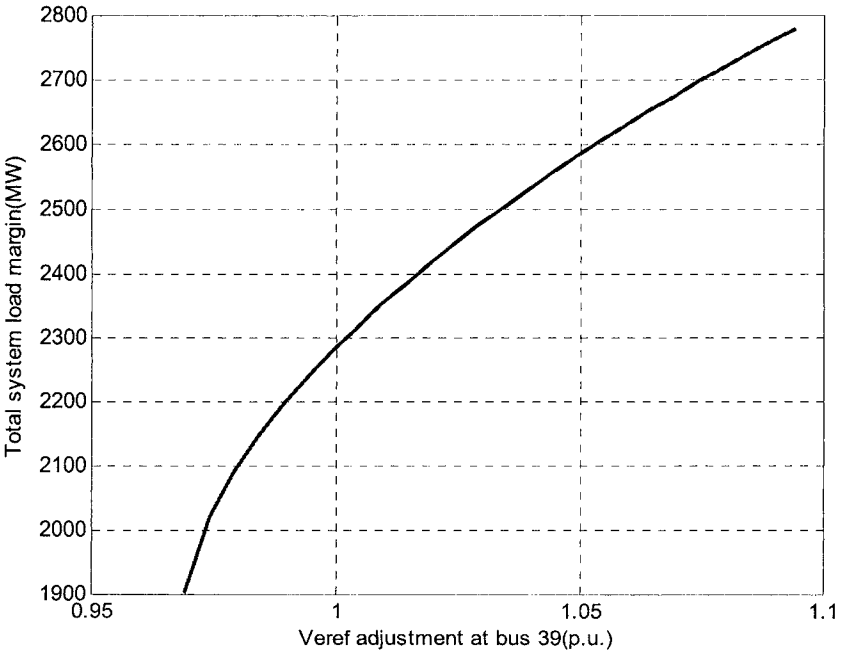

Fig. 5.10 System load margin vs. V_{ref} adjustment at generator bus 39

5.4.5 Control combination

The control scenario could be any combination of control parameters. Fig. 5.11 shows the variation of margin with simultaneous change in V_{ref}, and shunt compensation(The V_{ref} is increased from 1.084 p.u. to 1.092 p.u., and shunt capacitance is increased from 0 to 0.08 p.u.).

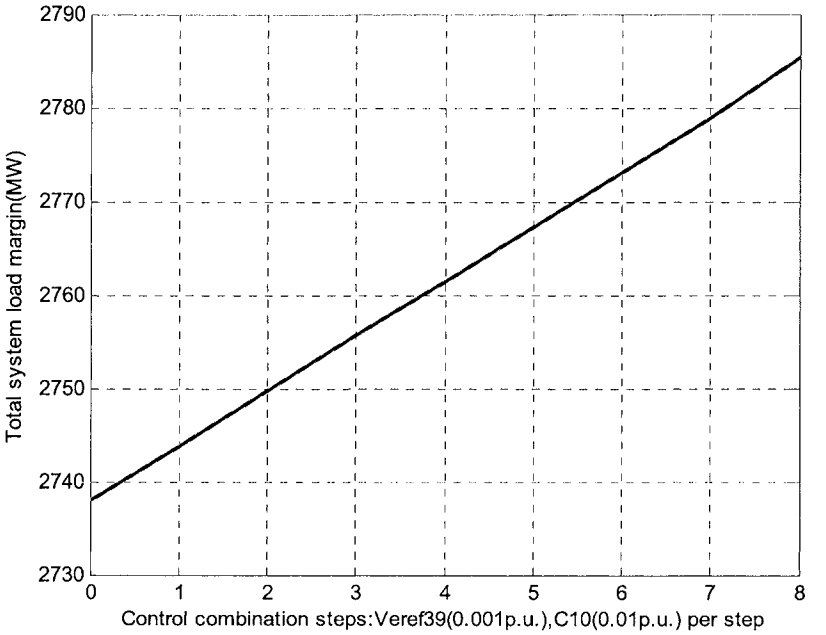

Fig. 5.11 System load margin vs. control combination steps: Vref39 (0.001pu), C10 (0.01pu)

5.4.6 Advantages of margin boundary tracing

- Margin Boundary Tracing is accurate and reliable.
- It is easy to take account of limit effects and other nonlinearities in Mar gin Boundary Tracing.
- Margin boundary tracing dramatically saves CPU time compare to obtaining each new boundary point by exhaustively recomputing the whole PV curve.

5.5 Formulation of Voltage Stability Limited ATC

Deregulation in power industries is promoting the open access of all transmission networks. However, this may lead to the violation of transfer capability in the networks. These aspects have motivated the development of methodologies to evaluate existing power transfer capabilities and transmission margins. The term "Available Transfer Capability" (ATC) [7]

is used to measure the transfer capability remaining in the physical transmission network for further commercial activity over already committed uses.

A key aspect in calculating ATC is the physical and operational limitations [7, 8] of the transmission system, such as circuit ratings and bus voltage levels. In addition, as power system become more heavily loaded, voltage collapse is more likely to occur.

To determine ATC is actually to determine TTC (Total Transfer Capability), which is the most critical physical or operational limit to the networks. TTC on some portions of the transmission network shifts among thermal, voltage and stability limits as the network operating conditions change over time. Fig.5.12 shows one possible ATC scenario with the low voltage limit is the critical constraint while in Fig.5.13 the voltage stability limit is the critical constraint [9].

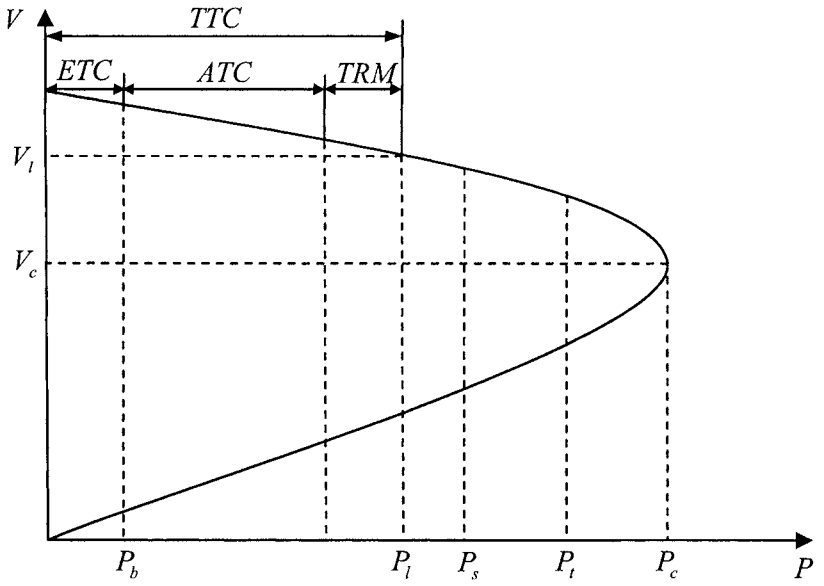

Fig.5.12 Illustration of ATC with low voltage limit as the critical constraint

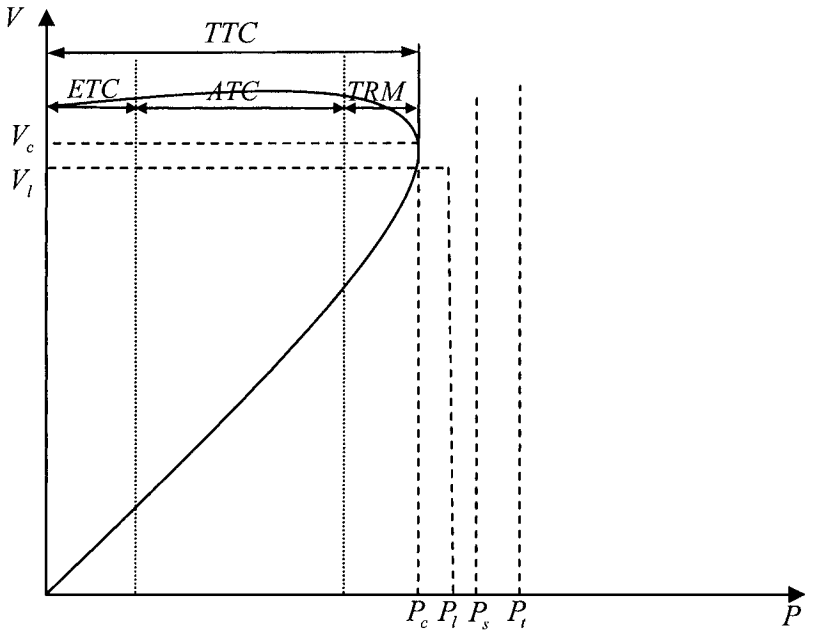

Fig.5.13 Illustration of ATC with voltage stability limit as the critical constraint

- V_l : Low voltage with respect to bus voltage limit;
- V_c : Critical voltage with respect to voltage collapse point;
- P_b : Existing Transmission Commitments (including CBM);
- P_l : Low voltage limit;
- P_s : Oscillatory stability or transient stability limit;
- P_t : Thermal overload limit;
- P_c : Voltage stability limit;
- TTC : $\min(P_l, P_s, P_t, P_c)$

The continuation power flow and the margin boundary tracing techniques can be applied to obtain voltage stability limited transactions.

For this we have to obtain scenario parameters that establish various transactions including multi-area simultaneous transactions. Next section describes how to obtain scenario parameters to establish a particular transaction.

5.6 Scenario Parameters

Recall equilibrium tracing introduced in chapter 3 is along a fixed load/generation changing pattern from the base case up to voltage collapse point. The load/generation changing pattern at each bus in the system is reproduced here for the continuity.

$$P_{Li}(\lambda) = P_{Li0} + \lambda K_{Li} P_{Li0} \tag{5.22}$$

$$Q_{Li}(\lambda) = Q_{Li0} + \lambda K_{Li} Q_{Li0} \tag{5.23}$$

$$\begin{aligned} P_{Gi}(\lambda) &= P_{Gi0} + K_{Gi} \sum_{i=1}^{N} (P_{Li}(\lambda) - P_{Li0}) \\ \sum_{i=1}^{N} K_{Gi} &= 1 \end{aligned} \tag{5.24}$$

Note that K_L s are not independent variables. They do not have any meaning if they are not compared to each other since K_{Li} only reflects the relative load change speed at one specific bus. For instance, if a system has only two buses where the load will increase, the case with $K_{L1} = 1$ and $K_{L2} = 2$ equals to the case where $K_{L1} = 2$ and $K_{L2} = 4$. In other words, it is the ratio between K_L s that determines the system active load increase scenario.

K_{Gi} reflects active generation dispatching pattern at each bus. When there is no generation increase at a particular bus *i*, the corresponding K_{Gi} is zero.

In summary, when the common λ increases, the active load, reactive load, and generation at each bus will increase at the rate determined by K_L s, and K_G s, respectively.

Keeping the essential meaning of K_L s, and K_G s in mind, we will see how they are extended in the following section to simulate the process of simultaneous multi-area transactions.

5.7 Scenario According to Simultaneous Multi-area Transactions

As shown in Fig.5.14, there is more than one desired transaction between n areas, which will take place at the same time. Since the n areas are interconnected, their performance will affect one another.

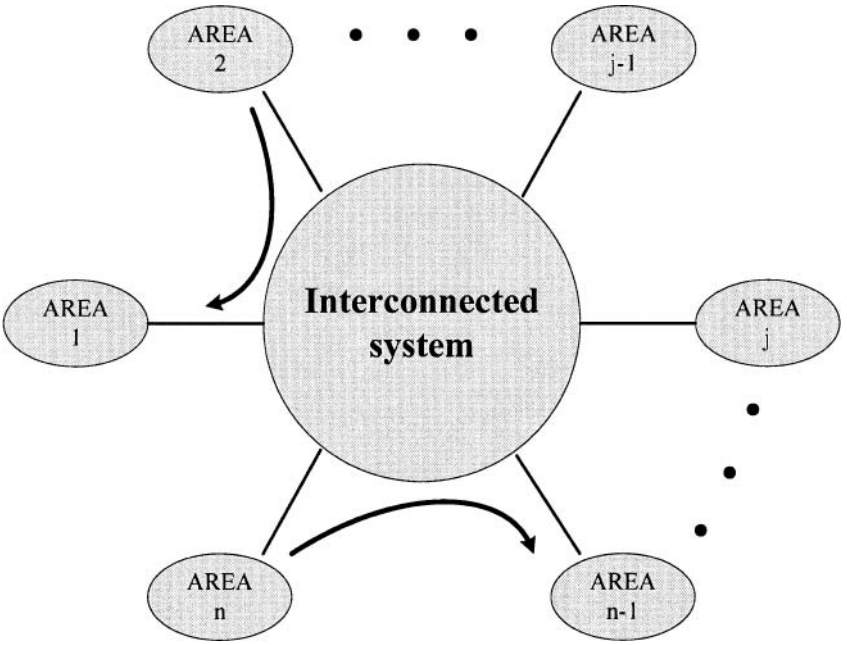

Fig.5.14 Multi-area transactions

In addition, one area may have several transactions with others at the same time either as seller or as buyer. For a highly meshed system, an explicit interface may not exist between areas. Thus choosing the interface flow to check whether these transactions are satisfied may not be reasonable. Alternatively, we can set up a criterion for judgment by checking the seller's supply and buyer's load increase. That is, according to the transactions associated to each area (either seller or buyer), we can summarize the total demand for each seller and requirement of each buyer. If at one point, each seller reaches its total supply demand while at the same time each buyer reaches its total requirement, we claim these transactions are satisfied simultaneously no matter how the flows go through the network. This criterion is also more suitable for studying voltage-stability-related problems since voltage stability is inherently related to system's load/generation pat-

tern, it cannot simply be judged by the flow over the transmission line like what is done to study thermal constraint.

Given the demand of each transaction between n areas (generalized in Table 5.2), we can obtain the total desired load demand for each area as well as the total desired generation supply for each area according to the transactions, which is shown in Table 5.3. For the sake of generality, we also consider transactions within the same area, e.g., i=j. Table 5.4 shows the total number of load increase buses and the total number of generation-sharing buses of each area.

Table 5.2 Transaction description

Area # of seller	Area # of buyer	Desired transaction amount (MW)
i	$j(j \neq i)$	P_{Tij}
i	i	P_{Tii}

Table 5.3 Demand for each area's generation and load

Area #	Demand for load (MW)	Demand for generation (MW)
1	$\sum_{i=1}^{n} P_{Ti1}$	$\sum_{i=1}^{n} P_{T1i}$
⋮	⋮	⋮
j	$\sum_{i=1}^{n} P_{Tij}$	$\sum_{i=1}^{n} P_{Tji}$
⋮	⋮	⋮
n	$\sum_{i=1}^{n} P_{Tin}$	$\sum_{i=1}^{n} P_{Tni}$

According to the information above, we need to determine the load parameters K_L s and generation parameters K_G s to simulate these transactions. For one-area case, scenario parameters can be set only according to the demand of load and generation at each bus in this particular area, without considering other area. So the load changing parameter, K_L s and generation changing parameter, K_G s can be determined arbitrarily as long as the total generation and load in the area can be balanced. However, for simultaneous multi-area transactions, merely using such strategy may cause a mismatch between the seller's actual generation and the corre-

sponding buyer's demand. Now that each area's scenario is considered within a combined large system, we need to guarantee the simultaneousness as well to match the seller's generation output to the corresponding buyer's load increase.

Table 5.4 Area scenario

Area #	Table # of generation increase buses	Total # of load increase buses
1	NG_1	NL_1
⋮	⋮	⋮
j	NG_j	NL_j
⋮	⋮	⋮
n	NG_n	NL_n

5.7.1 Determination of K_{Li}

According to the definition of simultaneous transactions, each area will increase its load in such a way that when it satisfies its own load demand according to transactions, other areas will also exactly satisfy their own load demand according to the transactions requirement. Without the loss of generality, we can assume that all involved areas increase their loads in a simultaneous way. That is, we can determine the load increase scenario according to the ratio of each area's load demand with respect to total load demand for the whole equilibria-tracing process from the base case, which guarantees the simultaneousness of a set of transactions.

Note that the load demand for each area (in Table 5.4) can be regarded as the net load increase from the base case for that particular area corresponding to the bifurcation parameter at that point, λ. Since we have defined the simultaneousness of the set of transactions, λ is common for each area, which can be mathematically expressed with the following equation set (compared to Eq.5.22):

$$\begin{aligned}
\lambda\sum_{k=1}^{NL_1} K_{Lk}^{(1)} P_{Lk0}^{(1)} &= \sum_{i=1}^{n} P_{Ti1} \\
&\vdots \\
\lambda\sum_{k=1}^{NL_j} K_{Lk}^{(j)} P_{Lk0}^{(j)} &= \sum_{i=1}^{n} P_{Tij} \\
&\vdots \\
\lambda\sum_{k=1}^{NL_n} K_{Lk}^{(n)} P_{Lk0}^{(n)} &= \sum_{i=1}^{n} P_{Tin}
\end{aligned} \tag{5.25}$$

where P_{Lk0} refers to the existing load at bus k and the upper note (j) specifies the area in which that bus resides.

By summarizing the left-hand-sides and right-hand sides of each equation in equation set 5.25, respectively, we have

$$\lambda\sum_{j=1}^{n}\sum_{k=1}^{NL_j} K_{Lk}^{(j)} P_{Lk0}^{(j)} = \sum_{j=1}^{n}\sum_{i=1}^{n} P_{Tij} \tag{5.26}$$

The right-hand-side of Eq.5.26 is nothing but the total transactions' demand. We simply denote it as follows:

$$P_{TOTAL} = \sum_{j=1}^{n}\sum_{i=1}^{n} P_{Tij} \tag{5.27}$$

Taking one equation related to AREA j from Eq.5.25 and dividing it by Eq.5.26, we get

$$\frac{\sum_{k=1}^{NL_j} K_{Lk}^{(j)} P_{Lk0}^{(j)}}{\sum_{j=1}^{n}\sum_{k=1}^{NL_j} K_{Lk}^{(j)} P_{Lk0}^{(j)}} = \frac{\sum_{i=1}^{n} P_{Tij}}{P_{TOTAL}} \tag{5.28}$$

We normalize K_L s by letting

$$\sum_{j=1}^{n}\sum_{k=1}^{NL_j} K_{Lk}^{(j)} P_{Lk0}^{(j)} = C \tag{5.29}$$

where C is an arbitrary constant in MW. Then Eq.5.28 is transformed to

$$\sum_{k=1}^{NL_j} K_{Lk}^{(j)} P_{Lk0}^{(j)} = C \frac{\sum_{i=1}^{n} P_{Tij}}{P_{TOTAL}} \tag{5.30}$$

Eq.5.30 reflects when the total systems' load changes; each area's load changes according to the fraction determined by the transactions.

The purpose of normalizing K_L s is mainly to keep bifurcation parameter λ and system transfer (in MW) consistent and make these two have simple mathematical relationship. Choosing C is arbitrary because it affects only the value of K_L s but not their essence (see Section 5.6).

To finally determine K_L s, we further need the load change relationship between each bus in a particular area, which can be given in the following form:

$$K_{L1}^{(j)} : \cdots : K_{Lk}^{(j)} : \cdots : K_{L,NL_j}^{(j)} = \mu_1^{(j)} : \cdots : \mu_k^{(j)} : \cdots : \mu_{NL_j}^{(j)} \tag{5.31}$$

where $\mu_k^{(j)}$ is a constant coefficient. By introducing a common variable for each area j, $K_{L\_BASE}^{(j)}$, we can transform Eq.5.31 to

$$\begin{aligned} K_{L1}^{(j)} &= \mu_1^{(j)} K_{L\_BASE}^{(j)} \\ &\vdots \\ K_{Lk}^{(j)} &= \mu_k^{(j)} K_{L\_BASE}^{(j)} \\ &\vdots \\ K_{L,NL_j}^{(j)} &= \mu_{NL_j}^{(j)} K_{L\_BASE}^{(j)} \end{aligned} \tag{5.32}$$

Substituting Eq.5.32 into 5.30, we get

$$K_{L\_BASE}^{(j)} = C \frac{1}{\sum_{k=1}^{NL_j} \mu_k^{(j)} P_{Lk0}^{(j)}} \frac{\sum_{i=1}^{n} P_{Tij}}{P_{TOTAL}} \tag{5.33}$$

Substituting Eq.5.33 into 5.32, we finally obtain K_L for each bus in each area as follows:

$$K_{Lk}^{(j)} = C\frac{\mu_k^{(j)}}{\sum_{k=1}^{NL_j}\mu_k^{(j)}P_{Lk0}^{(j)}}\frac{\sum_{i=1}^{n}P_{Tij}}{P_{TOTAL}} \tag{5.34}$$

Through the above procedure, the obtained K_Ls reflect the load change relationship between each bus strictly according to the transactions.

5.7.2 Determination of K_{Gi}

According the principle of simultaneous transactions, each generation area needs to pick up the load demand associated with it. From the whole system point of view, each generation area only picks up part of the total load demand. Thus we can assign the ratio of generation sharing for one particular area according to Table 5.3 as follows:

$$\sum_{k=1}^{NG_j}K_{Gk}^{(j)} = \frac{\sum_{i=1}^{n}P_{Tji}}{P_{TOTAL}} \tag{5.35}$$

Eq.5.35 shows that each generating area picks up part of total load according to the transaction associated with it. To finally determine $K_G^{(j)}$s, we further need the generation-sharing relationship between each bus in a particular area, which can be given in the following form:

$$K_{G1}^{(j)}:\cdots:K_{Gk}^{(j)}:\cdots:K_{G,GL_j}^{(j)} = \eta_1^{(j)}:\cdots:\eta_k^{(j)}:\cdots:\eta_{GL_j}^{(j)} \tag{5.36}$$

where $\eta_k^{(j)}$ is a constant coefficient that reflects the relative generation-pick up of one particular bus. By introducing a common variable for each area j, $K_{G\_BASE}^{(j)}$, we can transform Eq.5.36 to

$$\begin{aligned}
K_{G1}^{(j)} &= \eta_1^{(j)}K_{G_BASE}^{(j)} \\
&\vdots \\
K_{Gk}^{(j)} &= \eta_k^{(j)}K_{G_BASE}^{(j)} \\
&\vdots \\
K_{G,NG_j}^{(j)} &= \eta_{NG_j}^{(j)}K_{G_BASE}^{(j)}
\end{aligned} \tag{5.37}$$

Substituting Eq.5.37 into 5.35, we get

$$K_{G\_BASE}^{(j)} = \frac{1}{\sum_{k=1}^{NG_j} \eta_k^{(j)}} \frac{\sum_{i=1}^{n} P_{Tji}}{P_{TOTAL}} \tag{5.38}$$

Substituting Eq.5.38 into 5.37, we finally obtain K_G for each bus in each area as follows:

$$K_{Gk}^{(j)} = \frac{\eta_k^{(j)}}{\sum_{k=1}^{NG_j} \eta_k^{(j)}} \frac{\sum_{i=1}^{n} P_{Tji}}{P_{TOTAL}} \tag{5.39}$$

Furthermore, this methodology is also applicable to more general cases such as multiple transactions from one area or load and generation increase in the same area.

5.8 Numerical Example

The procedure described in Section 5.3 is implemented in the EQTP simulation to show the effectiveness of direct ATC tracing. Various control scenarios have been traced for voltage stability related ATC margin boundary. Simultaneous multi-area transactions are defined in the simulation to show their impact on ATC margin for different areas.

5.8.1 Description of the simulation system

The numerical results are based on New England 39-bus system. As shown in Fig.5.15, New England 39-bus system is divided into four areas. The general connection between them is shown in Fig.5.16.

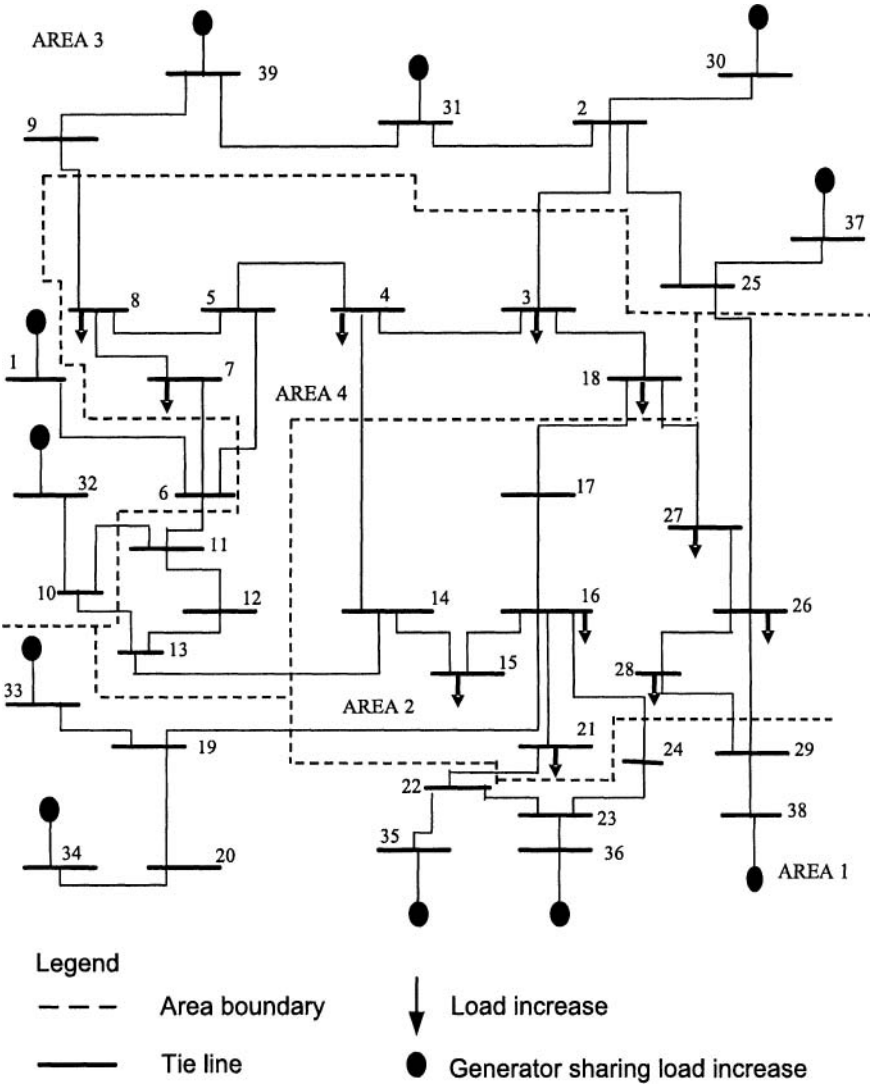

Fig.5.15 New England 39-bus system

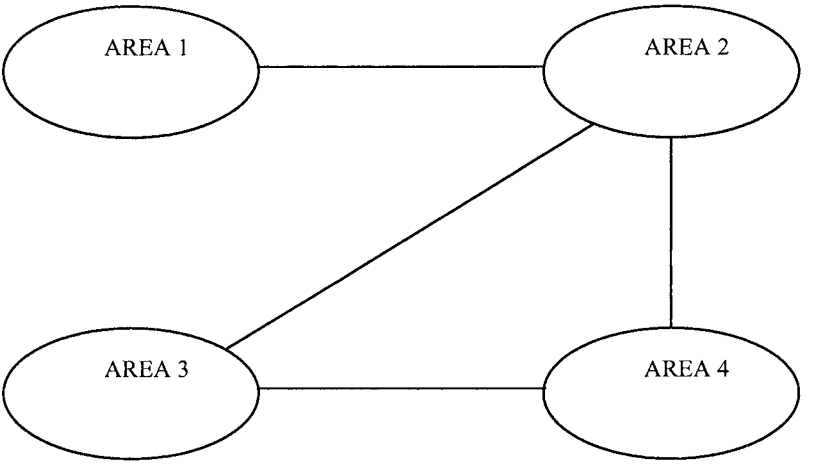

Fig.5.16 Illustration of area connection

There are two ATC scenarios considered in the simulation:

- One Transaction between AREA 1(seller) and AREA 2 (buyer);
- Two simultaneous transactions, one is between AREA 1 (seller) and AREA 2 (buyer), the other is between AREA 3 (seller) and AREA 4(buyer).

The load increase buses and generation sharing buses are listed in Table 5.5.

Table 5.5 Area scenario for New England 39-bus system

AREA #	Load Increase Bus	Generation Sharing Bus
1	None	33, 34, 35, 36, 38
2	15, 16, 21, 26, 27, 28	None
3	None	30, 31, 32, 37, 39
4	3, 4, 7, 8, 18	None

In the above ATC scenarios, the seller's generation should match its associated buyer's load demand. In the case of two simultaneous transactions, the amounts of transaction are proportional to the base case loads of corresponding areas.

The initial operation conditions of the areas are as follows:

Area 1:

Bus	Initial Real Generation (X100MW)	Power Factor
33	6.3	0.95 Leading
34	6.12	0.91 Leading
35	4.88	0.89 Leading
36	6.3	0.95 Leading
38	5.2	0.98 Leading
Total Generation	2880MW	

Area 2:

Bus	Initial Real Load (X100MW)	Power Factor
15	3.2	0.90 Lagging
16	3.294	0.93 Lagging
21	2.74	0.92 Lagging
26	1.39	0.95 Lagging
27	2.81	0.97 Lagging
28	2.06	0.99 Lagging
Total Load	1549 MW	

Area 3:

Bus	Initial Real Generation (X100MW)	Power Factor
30	2.3	0.71 Leading
31	7.23	0.93 Leading
32	6.3	0.92 Leading
37	5.2	0.99 Leading
39	10	0.99 Leading
Total Generation	3103 MW	

Area 4:

Bus	Initial Real Load (X100MW)	Power Factor
3	3.220	0.93 Lagging
4	5.000	0.94 Lagging
7	2.338	0.94 Lagging
8	5.220	0.95 Lagging
18	1.580	0.98 Lagging
Total Load	1736 MW	

Single Transaction:

In the single transaction example below, we determine the coefficients K_{Lk} according to (5.34)

$$K_{Lk}^{(j)} = C \frac{\mu_k^{(j)}}{\sum_{k=1}^{NL_j} \mu_k^{(j)} P_{Lk0}^{(j)}} \frac{\sum_{i=1}^{n} P_{Tij}}{P_{TOTAL}}$$

In (5.34), $\sum_{i=1}^{n} P_{Tij}$ is the total load in Area 2, which has the value 1549 MW; P_{TOTAL} is the total system load of the New England system, which has the value 6141 MW. According to the definition, P_{Lk0} is the existing load at bus k. Thus in this case, we have

$$P_{L15\_0} = 320 \quad P_{L16\_0} = 329.4 \quad P_{L21\_0} = 274$$
$$P_{L26\_0} = 139 \quad P_{L27\_0} = 281 \quad P_{L28\_0} = 206$$

Now the next job is to determine variable C and μ_k. Without loss of generality, we can define scalar C=1000. For variable μ_k, it defines load increment scenario in Area 2. And if the load is increased at various buses proportionally to their initial values, we have

$$\mu_{15} = \mu_{16} = \mu_{21} = \mu_{26} = \mu_{27} = \mu_{28} = 1$$

Finally we can calculate all the K_{Lk} in Area 2 with all these parameters:

$$K_{L15} = K_{L16} = K_{L21} = K_{L26} = K_{L27} = K_{L28}$$
$$= 1000 \times \frac{1}{320 + 329.4 + 274 + 139 + 281 + 206} \times \frac{1549}{6141} = 0.1628$$

Similarly, we can also define K_{Gk} according to (5.39). In (5.39), $\sum_{i=1}^{n} P_{Tji}$ is the total generation in Area 1, which has the value 3080 MW; and P_{TOTAL} is the same, 6141 MW. For variable η_k, it defines generation increment scenario in Area 1. And if the generation is increased at various buses proportionally to their initial values, we have

$$\eta_{33} : \eta_{34} : \eta_{35} : \eta_{36} : \eta_{38}$$
$$= P_{G33\_0} : P_{G34\_0} : P_{G35\_0} : P_{G36\_0} : P_{G38\_0}$$
$$= 630 : 612 : 488 : 630 : 520$$
$$= 0.2188 : 0.2125 : 0.1694 : 0.2188 : 0.1806$$

Finally, the coefficients K_{Gk} in area 1 can be calculated as follows:

$$K_{G33} = \frac{0.2188}{1} \times \frac{3080}{6141} = 0.1097$$

$$K_{G34} = \frac{0.2125}{1} \times \frac{3080}{6141} = 0.1066$$

$$K_{G35} = \frac{0.1694}{1} \times \frac{3080}{6141} = 0.0850$$

$$K_{G36} = \frac{0.2188}{1} \times \frac{3080}{6141} = 0.1097$$

$$K_{G38} = \frac{0.1806}{1} \times \frac{3080}{6141} = 0.0906$$

After rescaling K_{Gk} to make the sum equal to 1, we finally get:

$$K_{G33} = 0.2187 \quad K_{G34} = 0.2125 \quad K_{G35} = 0.1695$$
$$K_{G36} = 0.2187 \quad K_{G38} = 0.1806$$

In the single transaction, only area 1 and area 2 are involved. The load and generation conditions at the critical point are shown as follows:

Area 1:

Bus	Generation near the critical point (X100MW)	Power Factor
33	7.766	0.92 Leading
34	6.194	0.92 Leading
35	7.995	0.92 Leading
36	6.853	0.92 Leading
38	10.278	0.96 Leading
Total 1 Generation near the critical point	3909 MW	
Initial total Generation	3080 MW	
Generation Increment	829 MW	

Area 2:

Bus	Critical Load (X100MW)	Power Factor
15	4.879	0.90 Lagging
16	5.023	0.93 Lagging
21	4.178	0.92 Lagging
26	2.119	0.95 Lagging
27	4.285	0.97 Lagging
28	3.141	0.99 Lagging
Total Load at the critical point	2363 MW	
Initial total Load	1549 MW	
Load Increment	814 MW	

Simultaneous Transactions:

By the same way, we can also define the coefficients in simultaneous transactions. In this case, we still use (5.34) and (5.39) to determine these coefficients. And when applying (5.34) and (5.39) to determine Area 1 and Area 2 coefficients, we notice that all the parameters remain the same, thus we have the same coefficients of Area 1 and Area 2 as in the single transaction case.

As for the Area 3 and Area 4, we only need to know area 4 load and area 3 generation to apply (5.34) and (5.39). In this case, the area 4 load total is 1736 MW, and the area 3 generation total is 3103 MW. Thus, we can calculate the coefficients as follows:

For the load buses:

$$K_{L3} = K_{L4} = K_{L7} = K_{L8} = K_{L18}$$
$$= 1000 \times \frac{1}{322+500+233.8+522+158} \times \frac{1736}{6141} = 0.1628$$

For the generator buses:

$$\eta_{30} : \eta_{31} : \eta_{32} : \eta_{37} : \eta_{39}$$
$$= 230 : 723 : 630 : 520 : 1000$$
$$= 0.074 : 0.233 : 0.203 : 0.168 : 0.322$$

$$K_{G30} = \frac{0.074}{1} \times \frac{3103}{6141} = 0.037$$

$$K_{G31} = \frac{0.233}{1} \times \frac{3103}{6141} = 0.118$$

$$K_{G32} = \frac{0.203}{1} \times \frac{3103}{6141} = 0.103$$

$$K_{G37} = \frac{0.168}{1} \times \frac{3103}{6141} = 0.085$$

$$K_{G39} = \frac{0.322}{1} \times \frac{3103}{6141} = 0.163$$

After rescaling K_{Gk} to make the sum equal to 1, we finally get:

$$K_{G30} = 0.073 \quad K_{G31} = 0.233 \quad K_{G32} = 0.204$$
$$K_{G37} = 0.168 \quad K_{G39} = 0.322$$

In the simultaneous transactions, all 4 areas are involved. The load and generation conditions at the critical point are shown as follows:

Area 1:

Bus	Generation near the critical point (X100MW)	Power Factor
33	7.283	0.90 Leading
34	5.809	0.91 Leading
35	7.498	0.87 Leading
36	6.428	0.93 Leading
38	9.64	0.96 Leading
Total Generation near the critical point	3666 MW	
Initial total Generation	3080 MW	
Generation Increment	586 MW	

Area 2:

Bus	Critical Load (100MW)	Power Factor
15	4.371	0.90 Lagging
16	4.499	0.93 Lagging
21	3.742	0.92 Lagging
26	1.899	0.95 Lagging
27	3.838	0.97 Lagging
28	2.814	0.99 Lagging
Total critical Load	2116 MW	
Total Initial Load	1549 MW	
Load Increment	567 MW	

Area 3:

Bus	Generation near the critical point (X100MW)	Power Factor
30	2.785	0.88 Leading
31	8.751	0.89 Leading
32	7.626	0.89 Leading
37	6.287	0.91 Leading
39	12.107	0.96 Leading
Total Generation near the critical point	3756 MW	
Total Generation	3103 MW	
Generation Increment	653 MW	

Area 4:

Bus	Critical Load (X100MW)	Power Factor
3	4.398	0.93 Lagging
4	6.829	0.94 Lagging
7	3.193	0.94 Lagging
8	7.130	0.95 Lagging
18	2.158	0.98 Lagging
Total Critical Load	2371 MW	
Total Initial Load	1736 MW	
Load Increment	635 MW	

After ATC margin is calculated by the given scenarios, ATC margin change with respect to control resources can be calculated by the ATC tracing procedure described in Section 5.3. In the following numerical examples, the ATC margin change with respect to various control actions are given for both single transaction and simultaneous transactions.

Steps involved in tracing ATC as limited by voltage stability is described as follows:

1. Specify a transfer scenario, and calculate scenario coefficients according to (5.34) and (5.39).
2. Equilibrium Tracing Program (EQTP) starts at the current operating point for the initial ATC limit under fixed control configuration and specified transfer scenario.
3. Specify the control scenario that describes the change of control configuration or contingencies.
4. Change control parameter to new value βi, find the new initial starting point as shown in Fig. 5.1.
5. Use EQTP to trace the new ATC limit λ_i starting from the initial starting point in step 4.
6. Go to step 4 unless some control variables hit limits.

In the following sections, several numerical examples are given to show the ATC tracing procedure with respect to various controls. Two transaction scenarios; single and simultaneous transactions are considered. In the single transaction, power is transferred from area 1 to area 2, and the initial ATC limit is 814MW; while in the simultaneous transactions, power is transferred both from area 1 to area 2 and from area 3 to area 4, and the initial ATC limits are 567MW and 635MW respectively. Once the initial

ATC limit is calculated, control actions such as load relief, reactive power support, V_{ref} change are applied to directly trace the new ATC limit. The variations of ATC with respect to control actions are shown in the various figures below.

5.8.2 Emergency transmission load relief

In certain extreme conditions, transmission load relief (TLR) procedure is implemented to relieve overloading in the transmission system. Simulation has been done to find out the effectiveness of implementing TLR on certain buses.

5.8.2.1 Single transaction case

Fig.5.17 demonstrates the SNB related ATC margin change with TLR implemented at bus 7. At the base case, The SNB related ATC margin between AREA 1 and AREA 2 is 814MW. The SNB related ATC margin between AREA 1 and AREA 2 reaches its maximum 864MW when 140MW load is shed.

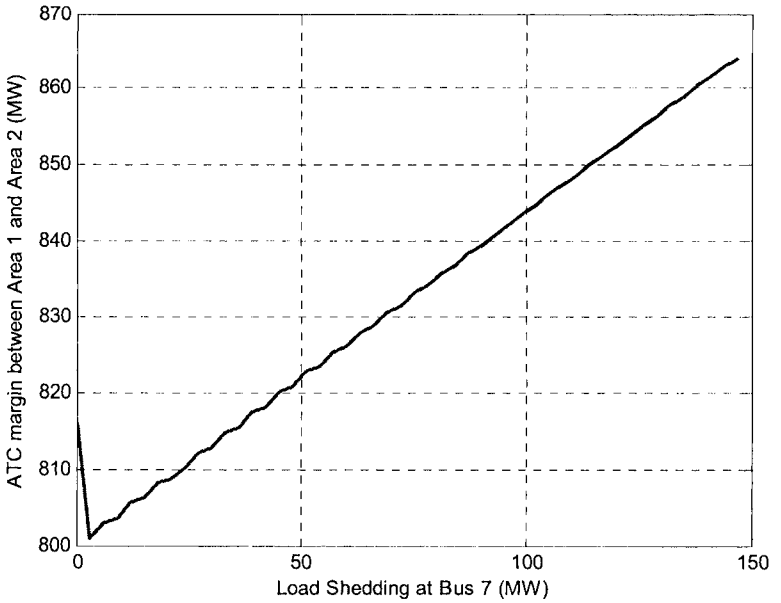

Fig.5.17 ATC margin vs. TLR implemented at bus 7 (single transaction)

5.8.2.2 Simultaneous transaction case

For the simultaneous transaction case, the amounts of power transfer for two transactions are proportional to each other according to the scenario setting. The seller's generation increase in AREA 1/AREA 3 matches the buyer's load increase in AREA 2/AREA 4 respectively. Fig.5.18 shows the voltage stability (SNB) related ATC margin change for both transactions. Along with the load shedding at bus 27, the SNB related ATC margin for both transactions increase from 567MW/635MW to 670MW/738MW respectively. The margin tracing curve is smooth and close to linear.

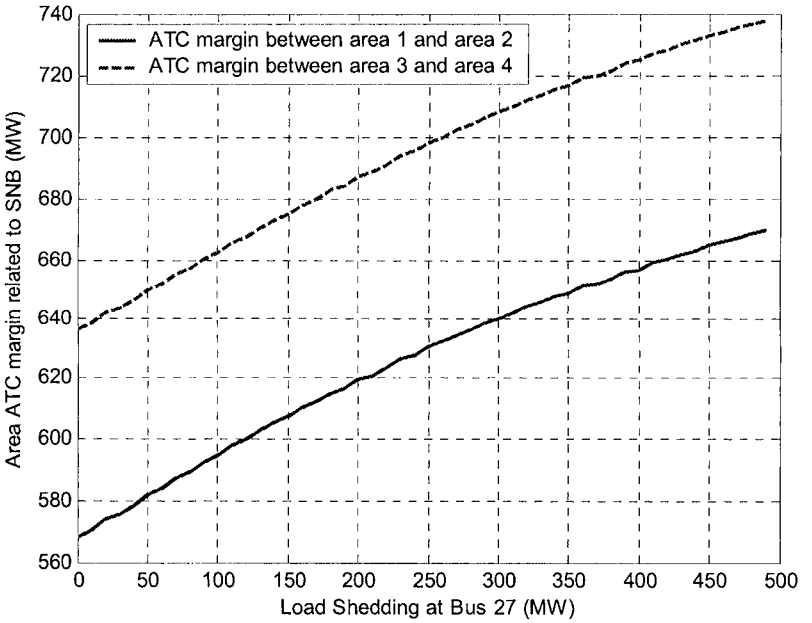

Fig.5.18 SNB related ATC margin vs.TLR implemented at bus 27 (simultaneous transaction case)

5.8.3 Reactive power Support

5.8.3.1 Single transaction case

Fig.5.19 shows the SNB related ATC margin change between AREA 1 and AREA 2 as shunt capacitance increases at bus 7. The ATC margin tracing

curves show the highly nonlinear characteristics and some "jumps" because of generators hitting their limits.

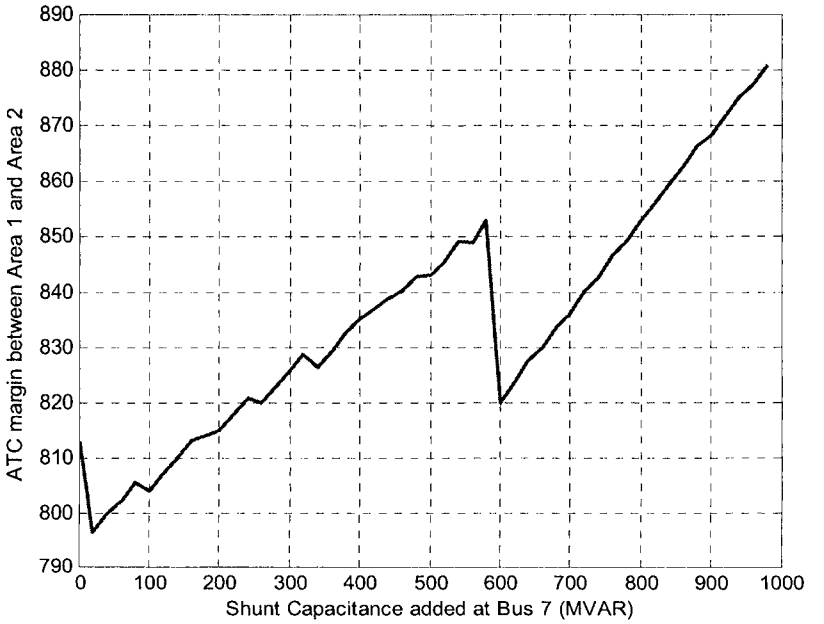

Fig.5.19 ATC margin vs. shunt capacitance at bus 7 (single transaction case)

5.8.3.2 Simultaneous transaction case

Fig.5.20 demonstrates the SNB related ATC margin change for simultaneous transactions as the shunt capacitance increases at bus 21. In Fig.5.20, the drop in stability margin at 300 MVAr shunt capacitance level is caused by generator 30 hitting its I_a and V_r limits.

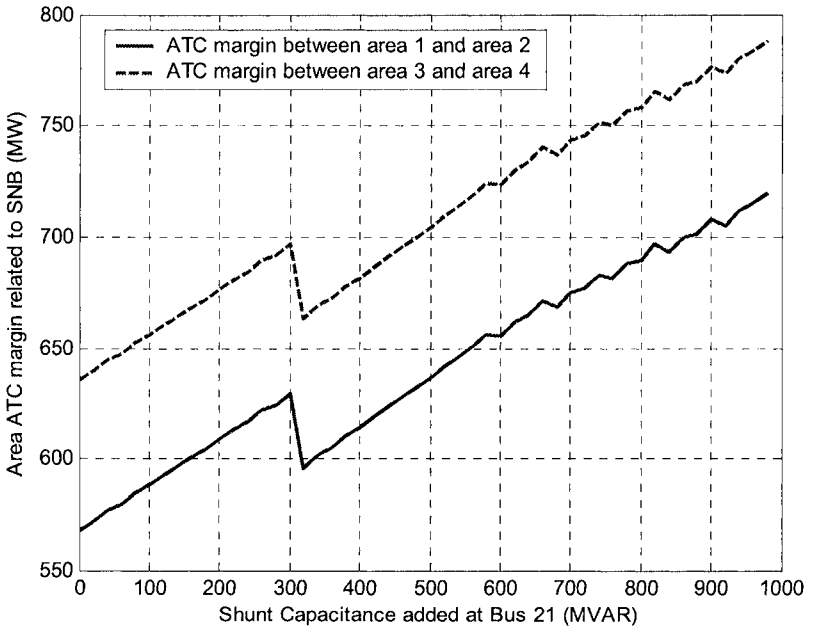

Fig. 5.20 SNB related ATC margin vs. shunt capacitance at bus 21 (simultaneous transaction case)

5.8.4 Control combination

The control scenario could be any combination of control parameters. The direct ATC tracing method can trace margin boundary with respect to the multi-control parameter space.

Fig.5.21 shows how the ATC margin changes with respect to a control scenario: At each step V_{ref} of generator 39 increases by 0.001 p.u; shunt capacitance at bus 31 increases by 0.1 p.u. and load shedding at bus 4 by 0.1 p.u. The control scenario simulates the total effect of secondary voltage regulation, as well as reactive power support and emergency TLR scheme.

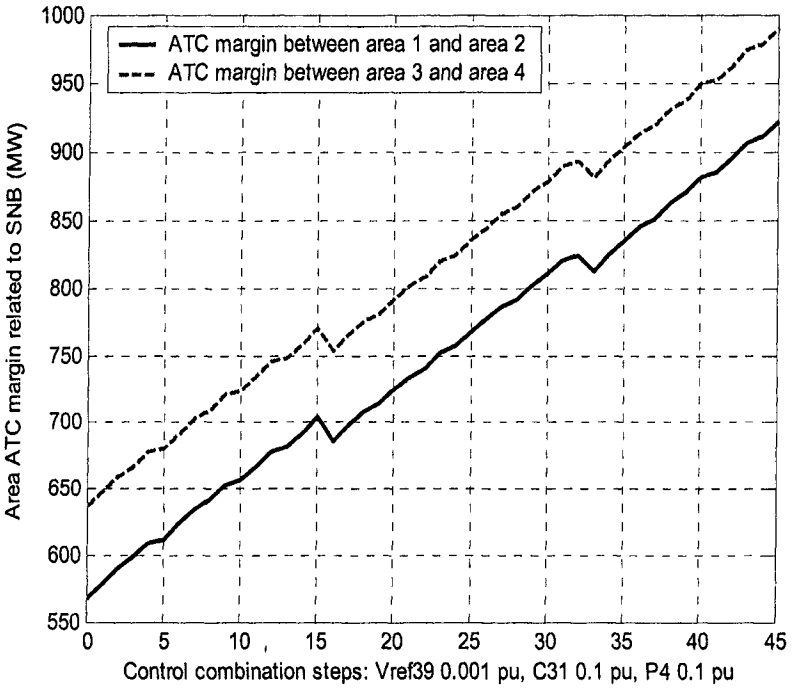

Fig.5.21 SNB related ATC margin vs. control combination (simultaneous transaction case)

5.9 Conclusion

In this chapter, the general framework of stability margin boundary tracing described in section 5.3 is reformulated to trace the voltage/oscillatory stability related ATC margin. The SNB related ATC margin boundary can be identified and traced along any control scenario combined with any given load/generation increase scenario.

The aim here is to demonstrate the application of continuation based technique for transfer capability calculation. Literature related to transfer margin and ATC can be found in references [10-12]. Ref [13] provides an excellent tutorial introduction to ATC with examples.

References

[1] Van Cutsem, T., An approach to corrective control of voltage instability using simulation and sensitivity. IEEE Trans. on power systems, Vol. 10: 616-622, 1995

[2] Flueck, A.J., Dondeti, J.R., "A new continuation power flow tool for investigating the nonlinear effects of transmission branch parameter variations,"*IEEE Trans. on power systems*, vol.15, no.1, pp.223-227, Feb. 2000

[3] Zhou, Y., *Manifold based voltage stability boundary tracing, margin control optimization and time domain simulation*, Ph.D. thesis, Iowa State University, Ames, IA, 2001

[4] Dai, R., Rheinboldt, W.C., "On the computation of manifolds of foldpoints for parameter-dependent problems," *SIAM J. Numer. Anal.*, Vol. 27, no.2, pp. 437-446, 1990

[5] Feng, Z., Ajjarapu, V., Maratukulam, D. J. , Identification of voltage collapse through direct equilibrium tracing. IEEE Trans. on Power System, Vol. 15, pp. 342-349, 2000

[6] Van Cutsem, T., Vournas, C., *Voltage stability of Electric Power Systems*, Kluwer Academic Publishers, Norwell, MA, 2003

[7] http://www.nerc.com/~filez/reports.html. Transmission transfer capability task force, Available transfer capability definitions and determination. North American electric reliability council, Princeton, New Jersey, 1996

[8] Austria, R. R., Chao, X. Y., Reppen, N. D., Welsh, D. E., Integrated approach to transfer limit calculations. IEEE computer applications in power: 48-52, 1995

[9] Wang, G., Voltage Stability Based ATC and Congestion Management for Simultaneous Multi-Area Transactions, M.S. Thesis, July 1998

[10] North American Electric Reliability Council, "Transmission Transfer Capability", May 1995.

[11] Ilic, M.D., Yoon, Y.T., Zobian, A., "Available transmission capacity (ATC) and its value under open access," IEEE Trans. on Power System, Vol. 12, no.2, pp. 636-645, 1997

[12] Greene, S., Dobson, I., Alvarado, F.L., "Sensitivity of transfer capability margins with a fast formula," IEEE Trans. on Power System, Vol. 17, no.1, pp. 34-40, Feb.2002

[13] http://www.pserc.cornell.edu/tcc/